Coordination Chemistry Reviews
190–192 (1999) 629–647

www.elsevier.com/locate/ccr

Correlations of the distribution of spin states in spin crossover compounds

H. Spiering [a,*], T. Kohlhaas [a], H. Romstedt [a], A. Hauser [b], C. Bruns-Yilmaz [a], J. Kusz [a], P. Gütlich [a]

[a] *Institut für Anorganische Chemie und Analytische Chemie, Universität Mainz Staudinger Weg 9, D-55099 Mainz, Germany*

[b] *Département de Chimie Physique, Université de Genève, Bâtiment des Sciences II, 30 Quai Ernest-Ansermet, CH-1211 Geneva 4, Switzerland*

Accepted 13 March 1999

Contents

Abstract

Short range correlations of the distribution of high spin (HS) and low spin (LS) states show up in thermal spin transition curves, decay curves of the light induced metastable HS state (LIESST state), and in structural features during the spin transitions. Correlations are due to short range interactions between the spin crossover molecules. Short range interactions may compete with omnipresent long range interactions and give rise to interesting spin transition phenomena. In this paper, the effect of correlations on the thermal spin transition in the mixed crystal system $[Fe_xZn_{1-x}(pic)_3]Cl_2 \cdot EtOH$ (pic = picolylamine) is discussed. In

---

* Corresponding author. Tel.: +49-6131-392703; fax: +49-6131-392990.
E-mail address: spiering@iacgu7.chemie.uni-mainz.de (H. Spiering)

PII: S0010-8545(99)00109-5

particular the step in the thermal transition curve is a direct consequence of such correlations. In addition, the decay of the metastable HS state of the pure iron compound at ca. 20 K can be significantly changed by preparing metastable HS states with a random distribution over the lattice sites. Both experiments could be well reproduced by Monte Carlo simulations. In the orthorhombic modification of the compound Fe[5NO_2-sal-N(1,4,7,10)]([2,2′-(2,5,8,11-tetraazadodeca-1,11-diene-1,12-diyl)4-nitrophenolato] (2-)-N2, N2′,N2″,N2‴,O1, O1′]Fe(II)) a commensurable superstructure has been found. This compound represents the first example of a stable infinite range correlation of the spin states over the lattice sites.

Keywords: Phase transition; Spin crossover; Correlation

1. Introduction

In the research field of magnetic phase transitions correlations between interacting magnetic moments have been subject to many experimental and theoretical studies [1]. In systems with short range interactions, correlations between the objects build up. In case of magnetic materials, these objects are the exchange coupled spins. In spin crossover cormpounds, the molecules which can change their spin state are the interacting centers. Here the interaction mechanism was not so clear, so that depending on different assumptions about the range of the interactions, different phenomenological theories have been developed. The variety of approaches worked out in the research field of magnetic phase transitions stimulated the adoption of theories to the spin crossover phenomenon implicitly assuming short range interactions which then were treated in the simplest approximation of mean field theory [2–7]. Also consequences of sublattice structures, as successfully introduced for the description of antiferromagnetic structures, have been explored in mean field theory [8–12]. With Monte Carlo simulations short range interaction schemes could be treated exactly [13–15]. The good agreement of mean field approaches with experimental data, especially with series of transition curves obtained from metal dilution over the whole concentration range of the spin changing molecules [16], pushed the idea of long range interactions between the spin changing molecules to be of importance. Long range interactions average over many neighbours and therefore do not give rise to correlations. In the limit of infinite range interactions mean field theory becomes exact and all correlation functions vanish.

The change of the spin state of the spin crossover molecule from LS to HS state is accompanied by an increase of volume and a change of shape. These changes are observed on the molecular level by an increase of bond lengths and on the macroscopic level by a change of the unit cell of the crystal.

Such lattice strains, as known from elasticity theory, give rise to long range and even infinite range interactions. This fact was first pointed out by Onishi and Sugano [17]. A volume change of a few molecules uniformly distributed over the crystal, by replacing atoms of different size or by the spin state change of spin crossover molecules, leads to an image pressure on the surface of the crystal. This pressure effectively interacts with all molecules in the crystal (independent of distances) by the same strength. In fact, the contribution of the elastic interactions has been studied in detail both theoretically [18,19] and experimentally by measuring elastic constants by Brillouin spectroscopy [20] and temperature dependent X-ray diffraction [21]. It turns out that the interaction constants obtained from transition curves of the metal dilution series in $[Fe_xZn_{1-x}(propyltetrazole)_6](BF_4)_2$ essentially are explained by the elasticity theory (about 80%), where the molecules are treated as point defects and the lattice as a homogeneous medium [22,23]. This approximation, however, does not describe well the interactions at short distances comparable with the size of the molecules.

After the discovery of the so called two step transitions [24–26], it became obvious that short range interactions and therefore correlations are not negligible. The two step transitions exhibit a plateau in the curve of the HS fraction plotted versus temperature around a HS fraction of 50%. For systems with equivalent sites there is no way to reproduce steps in the spin crossover transition curves in mean field theory. The studies of models which ad hoc introduced sublattices of HS and LS molecules have shown that the competition between an antiferromagnetic type of interaction between the sublattices and ferromagnetic type of interaction within the sublattices lead to phase diagrams with two step behaviour. Consequently, short range interactions had to be taken into account explicitly in addition to the long range elastic interactions.

The anomalous transition of the compound $[Fe(2\text{-}pic)_3]Cl_2EtOH$ (pic = picolylamine) and its metal dilutions with the corresponding Zn compound have been studied in great detail. The theoretical interpretation of the thermal spin transitions and lifetime measurements of laser excited metastable HS states in the tunnelling region at low temperatures on the basis of Monte Carlo calculations have provided good insight into the role of correlation in spin crossover compounds.

2. Interaction energy

The interaction energy between two lattice sites at positions i and j in the crystal lattice expressed by an expansion series is a sum of terms $P_iA_{ij}P_j^\dagger$, where P and A are generally tensors of increasing rank. A_{ij} depends on the distance between sites i, j. In the lowest order, for instance the exchange interaction between two magnetic ions with spin S_i and S_j the interaction matrix A_{ij} is a $(2S+1)\times(2S+1)$ matrix. In elasticity theory the interaction energy of point defects is considered. The quantities P and A are second and fourth rank tensors, respectively. $P_iA_{ij}P_j^\dagger$ describes the interaction between two elastic dipoles. As in Ising systems of spin $S = 1/2$, the quantities P in a spin crossover system have two values P^H and P^L for the HS and LS states, respectively. Both kinds of molecules (HS and LS), are described by point defects implying a misfit of the molecules to the lattice. The interaction energy between all molecules is the double sum:

$$E_{\mathrm{I}} = \frac{1}{2}\sum_{i \neq j} P_i A_{ij} P_j^{\dagger} \tag{1}$$

The point defects P^{H} and P^{L} are not accessible experimentally, their difference $P^{\mathrm{HL}} = P^{\mathrm{H}} - P^{\mathrm{L}}$ is obtained from the deformation of the crystal on going from the LS to the HS state and the elastic constants of the crystal [18]. But the general double sum of Eq. (1) can be rearranged by introducing the tensor difference P^{HL} in such a way, that we formally can speak of the interaction between molecules in the HS state only, where the tensor difference P^{HL} is attributed to each HS site. In order to obtain this equation the sum over all lattice sites N ($i, j = 1, \ldots, N$) is split by summing separately over the sites N_{H}, N_{L} in the HS and LS state, respectively, with indices i_{H}, i_{L}. In Eq. (2) the three sums corresponding to interactions between (HS, HS), (HS, LS), and (LS, LS) molecules is expressed by three new sums, where only the first one has the shape of an interaction term.

$$\begin{aligned} E_{\mathrm{I}} &= \frac{1}{2}\sum_{i_{\mathrm{H}} \neq j_{\mathrm{H}}} P^{\mathrm{H}}_{i_{\mathrm{H}}} A_{i_{\mathrm{H}} j_{\mathrm{H}}} P^{\mathrm{H}\dagger}_{j_{\mathrm{H}}} + \sum_{i_{\mathrm{H}} j_{\mathrm{L}}} P^{\mathrm{H}}_{i_{\mathrm{H}}} A_{i_{\mathrm{H}} j_{\mathrm{L}}} P^{\mathrm{L}\dagger}_{j_{\mathrm{L}}} + \frac{1}{2}\sum_{i_{\mathrm{L}} \neq j_{\mathrm{L}}} P^{\mathrm{L}}_{i_{\mathrm{L}}} A_{i_{\mathrm{L}} j_{\mathrm{L}}} P^{\mathrm{L}\dagger}_{j_{\mathrm{L}}} \\ &= \frac{1}{2}\sum_{i_{\mathrm{H}} \neq j_{\mathrm{H}}} P^{\mathrm{HL}}_{i_{\mathrm{H}}} A_{i_{\mathrm{H}} j_{\mathrm{H}}} P^{\mathrm{HL}\dagger}_{j_{\mathrm{H}}} + \sum_{i_{\mathrm{H}} \neq j} P^{\mathrm{HL}}_{i_{\mathrm{H}}} A_{i_{\mathrm{H}} j} P^{\mathrm{L}\dagger}_{j} + \frac{1}{2}\sum_{i \neq j} P^{\mathrm{L}}_{i} A_{ij} P^{\mathrm{L}\dagger}_{j} \end{aligned} \tag{2}$$

The third one, which runs over all lattice sites ($i, j = 1, \ldots, N$) with P^{L} attached to each site, is a constant contribution only shifting the energy reference level. The second sum does not depend on the individual HS site (i_{H})—the case of equivalent sites of the unit cell is considered—, since the sum over j runs over all lattice sites with the same value P^{L} Consequently this term is proportional to the number of sites in the HS state, so that it introduces a constant energy separation Δ_{HL} between the HS and LS state:

$$\Delta_{\mathrm{HL}} = P^{\mathrm{HL}}_{i_{\mathrm{H}}} \sum_{j \neq i_{\mathrm{H}}} A_{i_{\mathrm{H}} j} P^{\mathrm{L}\dagger}_{j} \tag{3}$$

In the case of mixed crystal systems with molecules containing the metal ion M, there are six interaction terms which have to be rearranged. The energy shift is the same, but the interaction between sites in the HS state and metal sites M with the quantities P^{HL} and $P^{\mathrm{ML}} = P^{\mathrm{M}} - P^{\mathrm{L}}$, respectively, have to be considered. P^{ML} is also experimentally accessible by comparison of the unit cells of the pure HS and LS compound with the one containing only M. The total interaction energy becomes

$$\begin{aligned} E_{\mathrm{I}} &= \frac{1}{2}\sum_{i_{\mathrm{H}} \neq j_{\mathrm{H}}} P^{\mathrm{HL}}_{i_{\mathrm{H}}} A_{i_{\mathrm{H}} j_{\mathrm{H}}} P^{\mathrm{HL}\dagger}_{j_{\mathrm{H}}} + \sum_{i_{\mathrm{H}} j_{\mathrm{M}}} P^{\mathrm{HL}}_{i_{\mathrm{H}}} A_{i_{\mathrm{H}} j_{\mathrm{M}}} P^{\mathrm{ML}\dagger}_{j_{\mathrm{M}}} + \sum_{i_{\mathrm{H}} \neq j} P^{\mathrm{HL}}_{i_{\mathrm{H}}} A_{i_{\mathrm{H}} j} P^{\mathrm{L}\dagger}_{j} \\ &= \frac{1}{2}\sum_{i_{\mathrm{M}} \neq j_{\mathrm{M}}} P^{\mathrm{ML}}_{i_{\mathrm{M}}} A_{i_{\mathrm{M}} j_{\mathrm{M}}} P^{\mathrm{ML}\dagger}_{j_{\mathrm{M}}} + \sum_{i_{\mathrm{M}} \neq j} P^{\mathrm{ML}}_{i_{\mathrm{M}}} A_{i_{\mathrm{M}} j} P^{\mathrm{L}\dagger}_{j} + \frac{1}{2}\sum_{i \neq j} P^{\mathrm{L}}_{i} A_{ij} P^{\mathrm{L}\dagger}_{j} \end{aligned} \tag{4}$$

The second line in Eq. (4) does not run over sites which change the spin state and therefore is the constant energy shift. The mean field or Bragg Williams approximation is obtained by attributing the average of P to all sites, according to $\bar{P} = x(\gamma_{\mathrm{H}} P^{\mathrm{H}} + (1 - \gamma_{\mathrm{H}}) P^{\mathrm{L}}) + (1 - x) P^{\mathrm{M}}$, x is the fraction of spin changing

Fe^{2+} molecules and γ_H their fraction in the HS state. A random distribution of metal ions is, of course, assumed. Inserting $\bar{P}$ into Eq. (1) represents the mean field interaction term as usually used in the free energy of spin crossover systems. The sum of tensors $\Sigma_{i \neq j} A_{ij}$ does not depend upon the fraction of sites (i.e. i_H, i_L, i_M) over which the sum is carried out. Taking i, j over all sites, the interaction energy is expressed by the average tensor $\bar{A} = 1/N^2 \Sigma_{i \neq j} A_{ij}$.

$$E_I^{BW} = N^2 \left[\frac{1}{2} x^2 \gamma_H^2 P^{HL} \bar{A} P^{HL\dagger} + x(1-x)\gamma_H P^{HL} \bar{A} P^{ML\dagger} + x\gamma_H P^{HL} \bar{A} P^{L\dagger} \right.$$
$$\left. + \frac{1}{2}((1-x)P^{ML} - P^{L}) \bar{A} ((1-x)P^{ML\dagger} - P^{L\dagger}) \right] \quad (5)$$

The a priori unknown energy shift $P^{HL}\bar{A}P^{L\dagger}$ is part of the energy difference between the LS vibronic ground state and the lowest vibronic HS state. This shift is determined from the transition curve of isolated noninteracting spin crossover molecules in highly diluted mixed crystals and is therefore considered as the true value Δ_{HL} of Eq. (3). In the spin crossover literature the mean field interaction is usually written as $E_I = x^2 N \Delta \gamma_H - x^2 N \Gamma \gamma_H^2$ such that

$$\Delta = -N P^{HL} \bar{A} P^{ML\dagger}$$
$$\Gamma = -\frac{1}{2} N P^{HL} \bar{A} P^{HL\dagger} \quad (6)$$

In order to go beyond mean field theory by a minimal correction, we start from the mean field solution and take into account specifically the interaction to nearest and next nearest neighbours in such a way, that their mean field contributions vanish. This procedure results in a minimal number of additional parameters. The indices j_Q, $Q = H$, M of Eq. (4) are split into two parts. A small number j_Q^v counting next $v = n$ and next nearest $v = nn$ neighbours only and a macroscopically large number j_Q^μ for the rest of the crystal sites. The constant energies are dropped in the following expression for the interaction energy:

$$E_I = \frac{1}{2} \sum_{i_H j_H^\mu} P_{i_H}^{HL} A_{i_H j_H^\mu} P_{j_H^\mu}^{HL\dagger} + \sum_{i_H j_M^\mu} P_{i_H}^{HL} A_{i_H j_M^\mu} P_{j_M^\mu}^{ML\dagger} + \sum_{i_H \neq j} P_{i_H}^{HL} A_{i_H j} P_j^{L\dagger}$$
$$+ \frac{1}{2} \sum_{i_H j_H^v} P_{i_H}^{HL} A_{i_H j_H^v} P_{j_H^v}^{HL\dagger} + \sum_{i_H j_H^v} P_{i_H}^{HL} A_{i_H j_M^v} P_{j_M^v}^{ML\dagger} \quad (7)$$

The first two sums starting at the third coordination sphere (next to *nn* neighbours) will be already close to the average over all crystal sites, so that they are well approximated by their mean field values. Since the mean field values of the two sums over the neighbours j_Q^v should vanish, the mean field E_I^{BW} of Eq. (7) is the same as of Eq. (5). The condition for the vanishing mean field contribution is obtained by replacing all P by the mean value $\bar{P}$.

$$\frac{1}{2} \sum_{i_H j_H^v} A_{i_H j_H^v} + \sum_{i_H j_H^v} A_{i_H j_M^v} = 0 \quad (8)$$

As a consequence of the fact that all sites are equivalent, the sum over the neighbours j^{v}_{M} at fixed i_{H} already vanishes. We take the interaction with all next $v = n$ and next nearest $v = nn$ neighbours to be the same. Then the $A_{i_{\mathrm{H}} j^{v}}$ are the same for different indices $j^{n} = j'^{n}$ and $j^{nn} = j'^{nn}$, respectively, and the tensors $A_{i_{\mathrm{H}} j^{v}}$ can be abbreviated by A^{v}. If z^{n} and z^{nn} are the number of next and next nearest neighbours the condition for vanishing mean field contribution gives

$$z^{n} \cdot A^{n} + z^{nn} \cdot A^{nn} = 0 \tag{9}$$

Denoting the interaction term $P^{\mathrm{HL}} A^{v} P^{\mathrm{HL}\dagger}$ by $-2J^{v}$, only one parameter J^{n} is introduced because J^{nn} is given by Eq. (3). The second interaction constant between a HS and a M-site $P^{\mathrm{HL}} A^{v} P^{\mathrm{ML}\dagger}$ will be close to J in the case of M = Zn, since the unit cells of the crystal in the HS state and the pure Zn crystal are very similar. For the compound under discussion the ratio $q = 0.8$ [19] of the mean field values $P^{\mathrm{HL}} \bar{A} P^{\mathrm{ML}\dagger} / P^{\mathrm{HL}} \bar{A} P^{\mathrm{HL}\dagger}$ fitted to the metal dilution series has been adopted for the short range interaction. The full interaction energy is thus given by

$$E_{\mathrm{I}} = x\gamma_{\mathrm{H}}(\Delta + \Delta_{\mathrm{HL}}) + x^{2} N \Delta \gamma_{\mathrm{H}} - x^{2} N \Gamma \gamma_{\mathrm{H}}^{2} - \sum_{\substack{r_i = n,nn, \\ i = i_{\mathrm{H}}}} J^{r_i} v_{\mathrm{H}}^{r_i} + q J^{r_i} v_{\mathrm{M}}^{r_i} \tag{10}$$

The first term proportional to $x\gamma_{\mathrm{H}}$ is an energy shift by $\Delta + \Delta_{\mathrm{HL}}$ of each HS molecule. This shift will later on be included in Δf_{HL}, the free energy difference between molecules in the HS and LS state in the absence of interaction. The energy shift proportional to x^{2} and the mean field interaction term depend linearly on the concentration x of spin crossover molecules in the metal diluted system. The sum collecting the contributions of short range interaction runs over all sites $i = i_{\mathrm{H}}$ in the HS state. $v_{\mathrm{H}}^{r_i}$ and $v_{\mathrm{M}}^{r_i}$ are the number of next ($r_i = n$) and next nearest ($r_i = nn$) molecules in the HS state and metal sites M, respectively. This expression for the interaction has been treated in the thermodynamical equilibrium by analytical methods by Romstedt et al. [27] and by Monte Carlo calculations. We present here the Monte Carlo calculations of the thermal transition curves and the relaxation curves at low temperatures from the metastable HS state to the LS ground state using identical parameters defined by Eq. (10).

3. Thermodynamic equilibrium

The first two-step transition with a plateau near the temperature $T_{1/2}$ (where $\gamma_{\mathrm{H}} = 1/2$) was discovered in [Fe(2-pic)$_3$]Cl$_2$·EtOH [24]. A more detailed study of the effects of metal dilution in the M = Zn series [Fe$_x$Zn$_{(1-x)}$(2-pic)$_3$]Cl$_2$·EtOH and on the behaviour of the transition under pressure was published later [28]. The step vanishes already for small Zn concentrations ($x \approx 0.9$) and under small external pressure of only 1 kbar, such that the transition can then be parameterised as a gradual one by a mean field free energy with parameters reasonably related to each other. This observation strongly indicates that the interactions between the spin changing ions is responsible for the step rather than some hidden inner degrees of freedom of the crystal lattice such as for example structural changes and soft modes.

Several early approaches in the literature went beyond mean field theory and allowed for correlations of the distribution of spin states. Approximate solutions for Ising systems were developed by Bethe [29] and Kramers–Wannier [30] which were systematically extended by a combinatoric method called cluster variation method by Kikuchi in the 1950s [31]. We have translated these methods using the concise nomenclature of Hijmans and De Boer [32] to spin crossover systems [33] and studied the effect of short range interactions on transition curves. Nowadays the Monte Carlo technique [34] is the easy way to treat an interaction Hamiltonian exactly.

The Hamiltonian of a system with HS and LS molecules—diluted in an isostructural matrix of M molecules—can be mapped on the well known problems of bond dilute Ising systems with quenched disorder [35]. There are two features which are special for spin crossover systems. These are the inner degrees of freedom of each Ising spin given by the vibronic energy levels of the molecules and the infinite range type of interactions between the molecules. The inner degrees of freedom are taken into account by replacing the energy separation between the two spin states of an isolated noninteracting molecule by the free energy difference $\Delta f_{\mathrm{HL}}(T)$ of the HS and LS state. This result is obtained by appropriately factorising the partition function of the Hamiltonian [36]. At $T = 0$ the free energy difference $\Delta f_{\mathrm{HL}}(T = 0)$ is just the energy difference ΔE_{HL}, between the lowest vibronic HS and LS states.

The Monte Carlo data were obtained using the standard importance sampling method with single spin flip kinetics [34] over a simple cubic $L*L*L$ lattice ($L = 20$) with periodic boundaries [37]. The number of nearest and next nearest neighbours are $z^{n} = 6$ and $z^{nn} = 12$. The sites of the Zn molecules were allocated at random and were fixed during simulation.

For the transition probability of a single spin flip the commonly used Metropolis function W_{M} was chosen:

$$W_{\mathrm{M}} \begin{cases} \dfrac{1}{\tau_s} & : \delta E < 0 \\[2ex] \dfrac{1}{\tau_s} \cdot \exp\left(-\dfrac{\delta E}{\mathrm{k}T} \right) & : \delta E \geq 0 \end{cases} \tag{11}$$

where τ_{s} is a time scale factor and δE the energy change by one spin flip. τ_{s} is arbitrary if thermal equilibrium only is considered. For an isolated noninteracting molecule $\delta E(\mathrm{LS} \rightarrow \mathrm{HS}) = \Delta f_{\mathrm{HL}}$. The energy difference including interactions is derived by considering the change of E_{I} if at one site a molecule changes from the LS to the HS state. The number of HS states $N_{\mathrm{H}} = x\gamma_{\mathrm{H}}N$ increases by 1. The difference $E_{\mathrm{I}}(N_{\mathrm{H}} + 1) - E_{\mathrm{I}}(N_{\mathrm{H}})$ of Eq. (5) gives $-2x\gamma_{\mathrm{H}}\Gamma - (1 - x)\Delta = \Delta_{\mathrm{HL}}$, for the long range contribution and $-\Sigma_{r = n,nn} J^{r} v^{r}_{\mathrm{H}} + qJ^{r} v^{r}_{\mathrm{Zn}}$ for the short range nearest and next nearest neighbour interactions of Eqs. (7) and (10), with the definitions given at the end of Section 2. v_Q^r, Q = H, Zn are the number of HS and Zn molecules in the $r = n$ nearest and $r = nn$ next nearest neighbour shell. Including all terms (independent of x and γ_H) in the free energy difference Δf_{HL} the Metropolis decision becomes:

$$\delta E(\text{LS} \rightarrow \text{HS}) = \Delta f_{HL} - 2x\gamma_H\Gamma + x\Delta - \sum_{r=n,nn} J^r v_H^r + qJ^r v_{Zn}^r \qquad (12)$$

Note that the LS state as the reference state does not appear in Eq. (12). The fraction of molecules in the HS state γ_H determines the long range interactions and has to be updated all the time.

For the simulations the mean field free energy fitting the diluted series ($x \leq 0.8$) was used [37]: $\Delta f_{HL}(T)$, $\Delta = 275\text{cm}^{-1}$, and $\Gamma = 175\text{cm}^{-1}$. In Fig. 1 the experimental and the simulated data of the metal (M = Zn) dilution series are plotted. The step of the transition curve is very sensitive to the concentration of Zn and already vanishes at $x = 0.9$. The simulated curves in Fig. 1 were calculated with the parameter $J^n = -17.4$ cm^{-1} fitted to the $x = 1$ transition curve. J^n, the sign of which is opposite to the long range interactions and J^{nn}, refers to an antiferromagnetic type of interaction.

The absolute value of the interactions with the nearest neighbour molecules is of comparable size with that of the long range interactions. For $z^n = 6$ neighbours the total interaction of about $|-105 \text{ cm}^{-1}|$ is 60% of Γ. Nevertheless, the appearance of a step in the transition curve sensitively depends on other parameters involved. Small pressure of the order of $p = 1$ kbar already suppresses the step in the transition curve as shown in Fig. 2. The energy shift of the HS state is equal to $p\delta v_{HL}$, where $\delta v_{HL} = 14$ Å^3 is the volume increase of the unit cell for each molecule

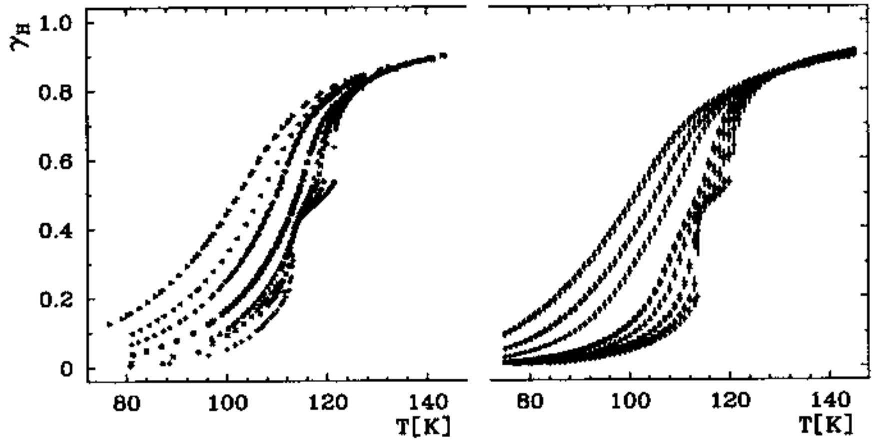

Fig. 1. The effect of metal dilution on the spin transition curve of $[Fe_xZn_{1-x}(2\text{-pic})_3]Cl_2 \cdot EtOH$ (x = 1.00, 0.98, 0.94, 0.89, 0.86, 0.70, 0.60, 0.50). The transition temperatures increase with increasing iron concentration x. The Monte Carlo simulations on the right hand side show the main features of the experimental data [28] on the left hand side.

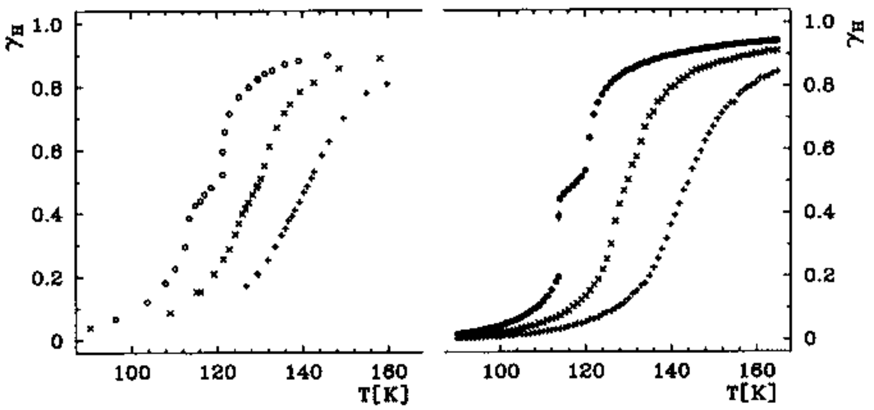

Fig. 2. The effect of pressure on the spin transition curve of $[Fe_xZn_{1-x}(2\text{-pic})_3]Cl_2{\cdot}EtOH$ ($p = 1.0$, 600, 1350 bar). The transition temperatures increase with increasing pressure. The Monte Carlo simulations on the right hand side show the main features of the experimental data [28] on the left hand side.

changing spin from LS to HS [38]. These shifts of $p\delta v_{HL} = 42$ and 95 cm^{-1} for $p = 600$ and 1350 bar, respectively, are small energies as compared to the range of energy separations in spin crossover molecules. The simulated transition curves in Fig. 2 again reproduce the observed behaviour of the transition curves.

The correlations between spin states can be analysed from the Monte Carlo samples in thermal equilibrium. The correlation length of an antiferromagnetic order has been estimated to be very short (for details see Ref. [39]), not larger than the next nearest neighbour distance. Therefore, an antiferromagnetic type of order over the whole crystal cannot be expected in agreement with X-ray measurements carried out in the temperature region of the step of the transition [40].

4. HS → LS relaxation

Relaxation measurements following laser excitation of the metastable HS state (LIESST [41]) under different irradiation conditions provided a direct proof of the formation of correlations in the spin crossover compound $[Fe(2\text{-pic})_3]Cl_2{\cdot}EtOH$. For infinite (long) range interactions, the decay rate does only depend on the fraction of molecules in the HS state:

$$\frac{d\gamma_H}{dt} = -k_{HL}(\gamma_H)\gamma_H \tag{13}$$

For the above mentioned system $[Fe(ptz)_6](BF_4)_2$, k_{HL} was found to depend exponentially on γ_H according to $k_{HL} = k_{HL}^0 \exp(-\alpha\gamma_H)$ leading to self-accelerated sigmoidal relaxation curves. In systems with strong short range interactions the decay probability of each individual complex will also depend on the spin state of the neighbouring molecules. As a result correlations may build up during the decay, and these, in turn, may change the decay probability of the whole system.

In spin crossover systems there is the unique possibility to prepare metastable HS states with a random distribution of spin states of any average HS fraction γ_H. The preparation of such a random distribution of spin states makes use of the fact that the excitation of a LS molecule by a photon is a random process. As long as the optical density at the irradiation wavelength is low enough so that there are no large intensity gradients of the exciting light inside the crystal, concentration gradients during the light induced HS → LS conversion are negligible. Fig. 3 shows the single crystal spectra of $[Fe(2\text{-pic})_3]Cl_2 \cdot EtOH$ before and after irradiation at 647 nm (15 456cm^{-1}), i.e. into the tail of the MLCT transition, using a Kr$^+$ laser. For this irradiation wavelength, the light induced LS → HS conversion takes only a short time (<1 min), as was confirmed by comparison of the HS bands after irradiation and at temperatures above the transition at 200 K (for details see Ref. [27]). From the spectra recorded at constant time intervals of 5 min at 23 K included in Fig. 3, the full HS → LS relaxation curve shown in Fig. 4a was extracted. The decay deviates strongly from single exponential with the rate increasing with increasing fraction of LS molecules at the beginning. The self acceleration region extends to $\gamma_H > 0.5$, at lower HS fraction the decay slows down considerably but still the rate is not constant. The dashed line represents the theoretical decay curve calculated in mean field theory as described below. The deviation from mean field theory becomes obvious at HS fractions $\gamma_H < 0.4$.

In order to prepare starting values lower than $\gamma_H(t=0)=1$, irradiation at 676nm (14 793cm^{-1}) close to the minimum optical density of the isosbestic point at 14 400 cm^{-1} was carried out. By varying the irradiation time (typically 5–15min at 5 mW laser power) $\gamma_H(t=0)$ could be adjusted from $0.1 < 1.0$. In Fig. 4b, the relaxation

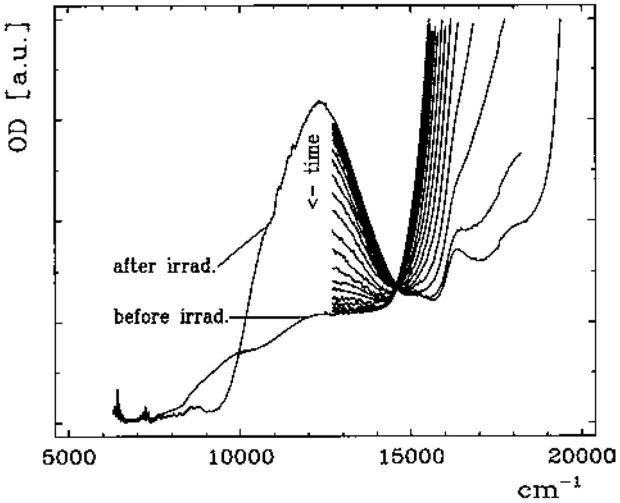

Fig. 3. Single crystal absorption spectra of $[Fe(2\text{-pic})_3]Cl_2 \cdot EtOH$ at $T = 23$ K before and after irradiation with light at 15 500 cm^{-1} and HS → LS relaxation spectra in time intervals of 5 min (→ increasing time of intervals) following irradiation [27].

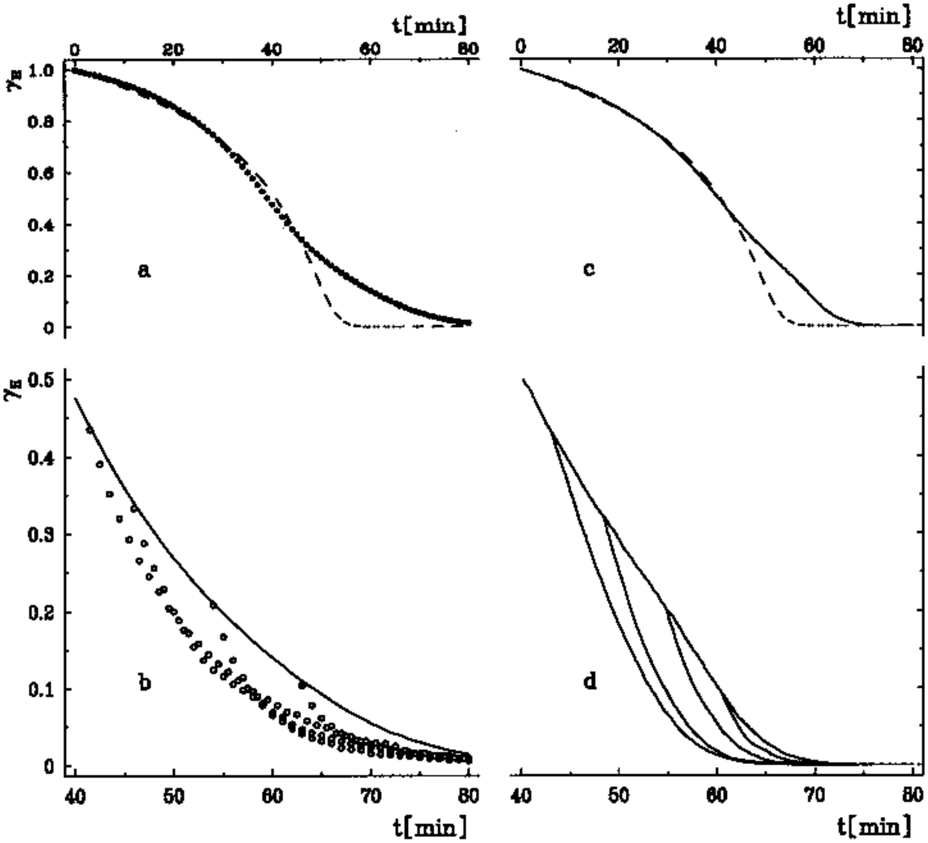

Fig. 4. HS → LS relaxation curves $\gamma_H(t)$ at $T = 23$ K for various starting values of the HS content $\gamma_H(t = 0)$. (a) The relaxation curve starting at $\gamma_H(t = 0) = 1.0$ (●). The dashed curve is calculated using mean field approximation. (b) Time shifted relaxation curves for $\gamma_H(t = 0) = 0.5$ (○) together with the decay curve $\gamma_H(t = 0) = 1.0$ from (a) as a reference represented by a *sp*line function. The corresponding simulated relaxation curves are plotted in (c), (d) [27]. The dashed line in (c) is the same as in (a).

curves for $\gamma_H(t = 0) < 0.5$ are plotted together with the $\gamma_H(t = 0) = 1$ curve as reference curve. The decay curves are shifted in time such that the $t = 0$ point matches the reference curve. Obviously, all these curves start off at a faster rate than the rate of the reference curve at the same HS fraction. We consider this observation as a direct proof of correlations building up during the decay. The findings are quantified in Fig. 5 using Eq. (13). The solid line is the *sp*line through the logarithm of the rate constants of the reference curve. A straight line (dashed) fits to the initial rates with starting values $\gamma_H(t = 0) < 0.5$.

These initial rates at different HS fractions are interpreted as rates belonging to a system with a random distribution of HS and LS molecules. Their dependence on the HS fraction is the same as was observed in the system $[Fe(ptz)_c](BF_4)_2$ mentioned above which could be well explained within the frame of mean field theory. The open triangles in Fig. 5 are initial rates calculated with the Monte Carlo method starting from a random distribution of HS and LS molecules.

For a treatment of dynamical processes the Metropolis function is an oversimplification for the complex processes in solid state determining the transition probabilities, so that the path through the large number of thermodynamical configurations selected by using the Metropolis function may be far from reality. In our case, however, the transition probability is well defined within the frame of the approximation used. In the tunnelling region the probability $W(\mathrm{HS} \rightarrow \mathrm{LS})$ depends on the energy separation ΔE_{HL}, between the lowest vibronic HS state and the LS ground state of the molecule in the crystal.

$$W(\mathrm{HS} \rightarrow \mathrm{LS}) \propto \exp(\eta \Delta E_{\mathrm{HL}}) \tag{14}$$

The probability for an excitation from LS to HS is negligible. In the approximation of a non adiabatic multi-phonon process in the limit of strong vibronic coupling the parameter $\eta \simeq \ln(S)/\hbar\omega$ depends on the Huang–Rhys parameter S, which is the reorganisation energy in units of the quanta $\hbar\omega$ of the active vibrational mode [42]. ΔE_{HL} is the energy separation of Eq. (12) at $T = 0$ K.

Correlation as well as random distribution of molecules in the HS state cause a distribution of energy separations by the short range interaction term in Eq. (12) and in turn a distribution of decay times. So the initial k_{HL} value for random distribution of HS states is an average rate constant and principally different from its mean field value. But it turns out that these average values within the frame of the theoretical approximations are very close to the mean field values.

Interpreting the slope $\alpha = -4.5$ of the dashed line fitting the initial decay rates as the slope calculated in mean field theory, the parameter η is fixed. The derivative

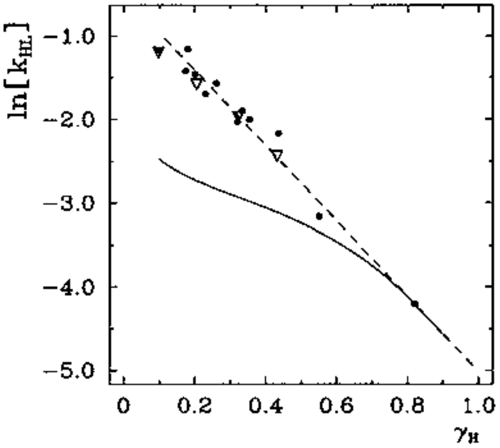

Fig. 5. Relaxation rate constants k_{HL} plotted as $\ln(k_{\mathrm{HL}})$ versus the HS fraction γ_{H}. The full circles are the rates at the starting values $\gamma_{\mathrm{H}}(t = 0)$. The solid line is a *sp*line function to the $\gamma_{\mathrm{H}}(t = 0) = 1.0$ curve. The slope of the straight dashed line to the full circles is $\alpha = -4.5$. The open triangles are theoretical initial rates from Fig. 4d. [27].

$d/d\gamma_H$ of the logarithm of k_{HL}, which is proportional to $W(HS \rightarrow LS)$, is directly obtained from Eq. (12), neglecting the short range interactions to be $\alpha = -2\eta\Gamma$.

Note that the resulting value of η is quite reasonable. Inserting $\Gamma = -175$ cm^{-1}, the definition of the Huang–Rhys factor $S = 1/2f(\Delta Q_{HL})2/\hbar\omega$ and values for Fe^{2+} ($\Delta Q_{HL} = \sqrt{6} \times 0.18$ Å, $f = 1.0105$ dyn cm^{-1}) [42], a frequency of $\hbar\omega = 290$ cm^{-1} for the active mode is derived, which is the value expected for the totally symmetric mode of the spin crossover molecule.

Now we are in the position to simulate decay curves by the Monte Carlo method. The rate of HS → LS transitions is defined by an adjustable scaling factor τ_{HL}:

$$k_{HL} = \frac{1}{\tau_{HL}} \exp(\eta \Delta E_{HL}) \tag{15}$$

The unknown time scaling factor was chosen large enough that the result did not depend on a further increase of τ_{HL}. Then the simulation is parameter free, this means that the parameters used for the simulation of thermodynamic equilibrium transitions were also used here without any adjustments. The result is shown in Fig. 4. In Fig. 4c the simulation with and without (dashed line) short range interactions are plotted. The short range interactions stabilise the HS state for HS fractions below $\gamma_H = 0.4$. The decay curves starting from random distribution at different HS fractions in Fig. 4d also show the characteristic features of the experimental one of Fig. 4b and the initial decay rates of these theoretical curves plotted as open triangles in Fig. 5 justify the whole procedure because they are close to the mean field values we started out with. Correlation lengths have been estimated in Ref. [27] to be less than two to three neighbouring spheres, which is of the same order as estimated in the step of the thermal transition.

5. Superstructure

The two step transition of [Fe(5NO_2-sal-N(1,4,7,10))] with a large step width of about 40 K, seemed to be a candidate for the observation of correlations of infinite range leading to a sublattice structure of HS and LS species [26] by X-ray diffraction. Boinard et al. [12] performed an X-ray diffraction study of this compound at different temperatures, above, below and inside the step, and claimed to have identified HS and LS sites of the unit cell inside the step. Some results of the X-ray measurements, however, are far out of the limits usually met for Fe(II) spincrossover molecules. The Fe–N bondlength to the nitrogen ligands typically vary by 0.1 Å for the LS state whereas Boinard et al. found a variation of 0.39 Å. Therefore we decided to repeat these measurements.

A modified preparation [43] of the compound revealed two modifications. One of them, A, had the spin transition properties as found by Petrouleas et al. [26], the spin transition curve of the other modification (B), Fig. 6, is mainly a gradual transition with a residual HS fraction of $\gamma_H(T = 0)$ close to 2/3. From both modifications, single crystals of sufficient size for X-ray measurements were obtained. The measurement on A did not confirm definite HS and LS sites in the unit

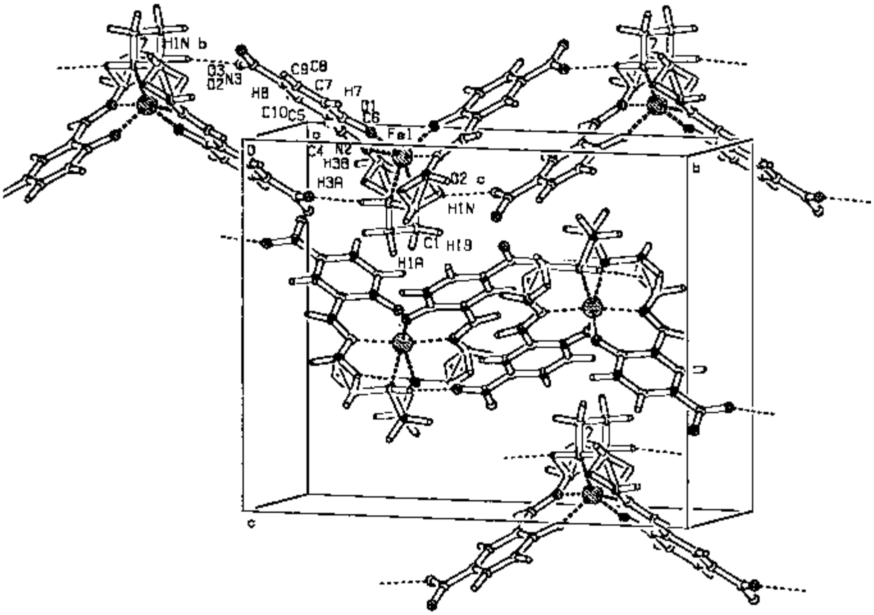

Fig. 6. Unit cell of the orthorhombic modification of [Fe(5NO$_2$-sal-N(1,4,7,10))]. The hydrogen bonds between the complex molecules are plotted as dashed lines.

cell of A. The correlation length is too small to be observed by X-ray measurements. In contrast to the result of Boinard et al. [12], we obtained no structural change accompanying the transition to the LS state of the compound.

The single crystal structure of A is the monoclinic one in the HS state as described by Boinard et al. [12]. The central iron atom is coordinated by six donor atoms of the dianion of the N_4O_2 ligand and is located on a two-fold symmetry axis. Due to the symmetry, space group $P2/c$ ($Z = 2$, $a = 10.153$ Å, $b = 8.490$ Å, $c = 13.173$ Å, $\beta = 109.93°$), the unit cell can be described with half a molecule (see Fig. 7). The two molecules in the unit cell are enantiomorphic and linked by hydrogen bonds, so that infinite chains of alternate enantiomorphic molecules are built. The two different Fe–N bondlength are 2.127 and 2.235 Å [12] in HS state at room temperature. In the LS state at 117 K we found 1.927 and 2.033 Å [43], respectively, which are in agreement with the typical decrease of 10%.

The modification B, however, exhibits a superstructure below 195 K. At room temperature the unit cell is orthorhombic. The orthorhombic unit cell is shown in Fig. 6. The compound crystallizes in the space group $Pccn$ with $Z = 4$ and $a = 7.083(1)$ Å, $b = 19.373(1)$ Å, $c = 15.270(1)$ Å. The orthorhombic structure is built up of the same chains as the monoclinic structure. In the upper part of Fig. 6, a chain is indicated by three molecules. The molecules are doubly hydrogen bonded, linking the secondary amine function of each complex to the terminal 5-nitro group of the neighbouring molecule (H1N– – – O3). In both structures the chains are arranged parallel in planes but the stacking of the planes are quite different. In the monoclinic structure the planes are related to each other by translational symmetry. In the orthorhombic structure adjacent planes are related by a mirror plane and a rotation normal to the plane by an angle of 40.2° about the *c*-axis.

Below 195 K the unit cell dimensions in the *a*- and *b*-directions become three times larger, 3*a* and 3*b*, and remain the same in the *c*-direction. The growth of the superstructure could be scanned by measuring several satellites of weak intensity. The superstructure could not yet be solved, so that there is no strict proof for the presence of a sublattice of LS sites. But a temperature dependent scan of the width of some reflections yields a good indication that such a lattice is formed. In Fig. 8 the width of the (− 902) reflection is plotted versus temperature. At the steep part of the spin transition at 195 K, the width steeply increases as a result of smaller LS molecules present in the lattice, which may already form sufficiently large domains in the crystal. The typical fluctuation time of microseconds fix the state of a molecule to a site in thermodynamical equilibrium only for short times of this order of magnitude. The intensity of the satellite reflection at the bottom of Fig. 8 is still close to zero. With decreasing temperature the LS fraction increases but the width of the (− 902) reflection decreases indicating growing domains of the new structure in the crystal. The increasing intensity of the satellite tells us that the domains forming a superstructure become dominant.

The striking effect is that at 160 K, when about 1/4 of the HS molecules have been converted to the LS state, the width decreases to the value of the crystal being completely in the HS state which is free of formation of domains of different lattice constants caused by molecules of different size. At the same temperature the satellites reach their full intensity. The simplest explanation for both observations is an ordered arrangement of the LS molecules at that temperature. On further lowering the temperature, the width increases again due to the increase of the fraction of LS molecules away from the fraction 1/4.

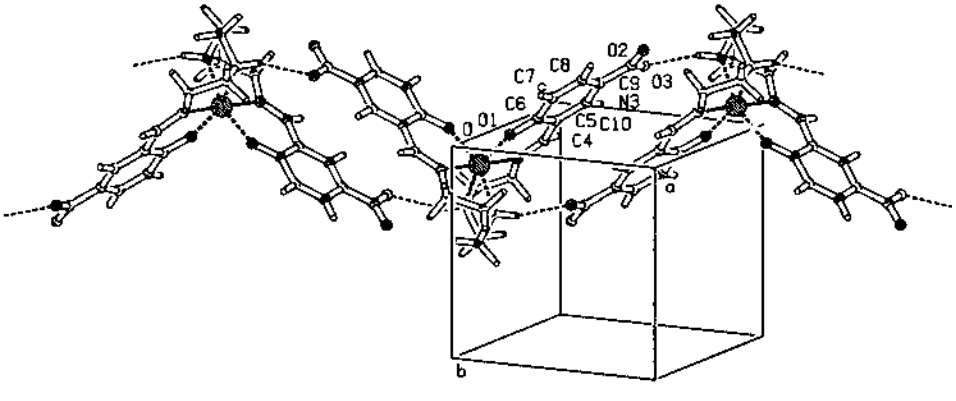

Fig. 7. Unit cell of the monoclinic modification of [Fe(5NO$_2$-sal-N(1,4,7,10))].

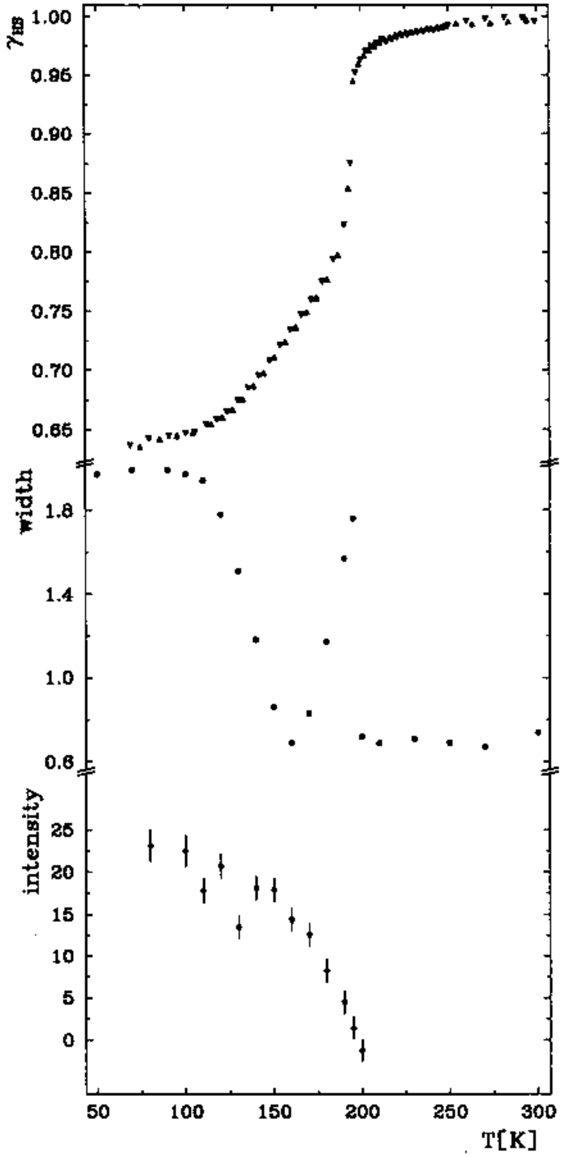

Fig. 8. HS fraction γ_H, the width of the (*hkl* = −902) reflection, and the intensity of the satellite reflection (*hkl* = 2113) of [Fe(5NO$_2$-sal-N(1,4,7,10))] versus temperature. The HS fraction has been measured with decreasing (▽) and increasing (△) temperature.

The corresponding isomorphous Zn compound has no superstructure, a fact which also supports the idea that the spin crossover phenomenon is responsible for the formation of a superstructure and at the LS fraction of 1/4 LS molecules occupy well defined sites in the enlarged unit cell.

6. Discussion

Although there was no evidence for correlations in spin crossover systems for a long time many theoretical approaches started from a microscopic picture where in a similar fashion to exchange coupled spins, only a short range interaction was introduced. Eventually, the mean field approximation was applied, and the equations derived for simulating and fitting experimental data were the same as those starting with long or even infinite range interactions, which are known as image pressures on free surfaces in elasticity theory [18,44]. The small step in the thermal transition curve of $[Fe(2\text{-}pic)_3]Cl_2{\cdot}EtOH$ was the first example which could not be understood in mean field theory. At that time, however, the beginning of the 1970s, there was no experience with this type of organometallic material, especially the dependence of their elastic properties on pressure and volume change during the spin transition, was unknown. The coupling of inner degrees of freedom of the crystal to the spin crossover system represented by the intramolecular vibronic states and the elastic interaction between them could have required a complete lattice theory such that an understanding of the step would have become out of range. From detailed metal dilution studies [28], it became clear that the spin crossover system itself produces the step and the lattice with its intermolecular properties remains stable. The first step was simulated for dimeric complexes of $[Fe(bt)(NCS)_2]_2(bpym)$ [25] where an asymmetric energy level scheme for the three states (HS–HS, HS–LS, and LS–LS) was introduced such that the HS–LS configuration is stabilised in energy. By this observation it became clear that an antiferromagnetic type of short range interaction is responsible for the anomalous thermal spin transitions. On the basis of this idea the broad step of about 40 K in $[Fe(5NO_2\text{-}sal\text{-}N(1,4,7,10))]$ has been simulated [45], assuming HS and LS sublattices with a ferromagnetic type of interaction within and an antiferromagnetic type between the sublattices as is the successful picture modelling antiferromagnetic compounds and their behaviour in applied magnetic fields.

The competition between ferromagnetic and antiferromagnetic type of interaction obviously leads to anomalous transitions. The long range elastic interaction is of ferromagnetic type, short range interactions may have either sign. The strength of long range interaction depends on the elastic properties and the change of volume and shape of the crystal during the spin transition. These quantities are always of similar size so that an upper limit of few hundred wavenumbers can be estimated for the long range interaction, which were found to be less than 200 cm^{-1} in all cases. Short range interactions are difficult to estimate. If for short distances (10 Å), elasticity theory is applied (which assumes a homogenous medium) values of ± 30–40 cm^{-1} dependent on the orientation of the elastic dipoles, have been obtained with the crystal properties of $[Fe(ptz)_c](BF_4)_2$ [22]. These values are even larger than $J^n = -17.5 cm^{-1}$ used to simulate the step. The question arises whether simulations of similar quality can also be obtained with larger short range at the expense of long range interactions. A decision may be possible if the metal dilution series over the whole range of concentration x is considered provided that the interaction scheme in the Monte Carlo algorithm is closer to the actual situation concerning the number and orientation of the nearest and next nearest neighbours. However, the fact that three situations are well reproduced, thermal equilibrium, the full decay curve with build up correlations, and initial decay rates at different HS fractions with random distribution of spin states, gives some confidence to the order of magnitudes obtained.

Large short range interaction constant may be expected if the metal ions are connected by bridging ligands as is observed in the dimeric complex mentioned or by strong hydrogen bridges between ligands. This is the case for the compound [Fe(5NO_2-sal-N(1,4,7,10))] where a superstructure has been observed. The structure is build up of chains with hydrogen bonds as connections so that the LS sublattice are likely along these chains.

Acknowledgements

This work was financially supported by the Deutsche Forschungsgemeinschaft (DFG), the Materialwissenschaftliches Forschungszentrum der Universität Mainz, the Fonds der Chemischen Industrie, the Schweizerische Nationalfonds, and the research fund TMR of the European Community under contract Nr. ERBFMRX-CT980199.

References

[1] C. Domb, M.S. Green (Eds.), Phase Transitions and Critical Phenomena, Academic, London, 1972.

[2] J. Wajnflasz, Phys. State Solids 40 (1970) 537.

[3] C.P. Slichter, H.G. Drickamer, J. Chem. Phys. 56 (1972) 2142.

[4] T. Kambara, J. Chem. Phys. 70 (1979) 4199.

[5] T. Kambara, J. Phys. Soc. Jpn. 49 (1806) 1980.

[6] G. Lemercier, A. Bousseksou, S. Seigneuric, F. Varret, J.-P. Tuchagues, Chem. Phys. Lett. 226 (1994) 289.

[7] H. Bolvin, O. Kahn, Chem. Phys. 192 (1995) 295.

[8] R.A. Bari, J. Sivardière, Phys. Rev. B 5 (1972) 4466.

[9] N. Sasaki, T. Kambara, Phys. Rev. B 40 (1989) 2442.

[10] A. Bousseksou, J. Nasser, J. Linares, K. Boukheddaden, F. Varret, J. Phys. I Fr. 2 (1992) 1381.

[11] B.G. Vekhter, J. Appl. Phys. 75 (1994) 5863.

[12] D. Boinard, A. Bousseksou, A. Dworkin, J.M. Savariault, F. Varret, J.P. Tuchagues, Inorg. Chem. 33 (1994) 271.

[13] K. Takahashi, Z. Phys. B Condens. Matter 71 (1988) 205.

[14] J. Linares, J. Nasser, A. Bousseksou, K. Boukheddaden, F. Varret, JMMM 140 (1995) 1503/1507.

[15] J. Linares, Oral Communication, El Saler, Valencia, 1995.

[16] M. Sorai, J. Ensling, P. Gutlich, Chem. Phys. 18 (1976) 199.

[17] S. Ohnishi, S. Sugano, J. Phys. C Solid State Phys. 14 (1981) 39.

[18] N. Willenbacher, H. Spiering, J. Phys. C 21 (1988) 1423.

[19] H. Spiering, N. Willenbacher, J. Phys. Condens. Matter 1 (1989) 10089.

[20] J. Jung, F. Bruchhäuser, R. Feile, H. Spiering, P. Gutlich, Z. Phys. B 100 (1996) 517.

[21] L. Wiehl, H. Spiering, P. Gutlich, K. Knorr, J. Appl. Cryst. 23 (1990) 151.

[22] J. Jung, Two aspects of elasticity in the spin crossover compound $[Fe_xZn_{1-x}(ptz)_6](BF_4)_2$, Ph.D. Thesis, D77, Johannes-Gutenberg Universität, Mainz, 1995.

[23] J. Jung, G. Schmitt, A. Hauser, L. Wiehl, K. Knorr, H. Spiering, P. Gütlich, Z. Phys. B 100 (1996) 523.
[24] H. Köppen, E.W. Müller, C.P. Köhler, H. Spiering, E. Meissner, P. Gütlich, Chem. Phys. Lett. 91 (1982) 348.
[25] J.A. Real, B. Gallois, T. Granier, F. Suez-Panama, J. Zarembowitch, Inorg. Chem. 31 (1992) 4972.
[26] V. Petrouleas, J.-P. Tuchagues, Chem. Phys. Lett. 137 (1987) 21.
[27] H. Romstedt, A. Hauser, H. Spiering, J. Phys. Chem. Solids 59 (1998) 265.
[28] C.P. Köhler, R. Jakobi, E. Meissner, L. Wiehl, H. Spiering, P. Gütlich, J. Phys. Chem. Solids 51 (1990) 239.
[29] H.A. Bethe, Proc. R. Soc. Lond. A135 (1935) 552.
[30] H.A. Kramers, G.H. Wannier, Phys. Rev. 60 (1941) 252.
[31] R. Kikuchi, Phys. Rev. 81 (1951) 988.
[32] J. Hijmans, J. De Boer, Phyisica 21 (1955) 471.
[33] H. Romstedt, H. Spiering, P. Gütlich, J. Phys. Chem. Solids 59 (1998) 1353.
[34] K. Binder, D.W. Heermann, Monte Carlo Simulation in Statistical Physics, Springer, Berlin, 1988.
[35] W. Selke, L.N. Shchur, A.L. Talapov, Annual Reviews of Computational Physics, vol. 1, World Scientific, Singapore, 1995.
[36] T. Kohlhaas, H. Spiering, P. Gütlich, J. Phys. Chem. Solids 59 (1998) 1353.
[37] T. Kohlhaas, H. Spiering, P. Gütlich, Z. Phys. B 102 (1997) 455.
[38] E. Meissner, H. Köppen, H. Spiering, P. Gütlich, Chem. Phys. Lett. 95 (1983) 163.
[39] T. Kohlhaas, Computersimulation des thermischen Spinühergangs mit Stuie 1bei Fe(II)-Komplezen, Master's Thesis, Johannes-Gutenberg Universität, Mainz, 1995.
[40] L. Wiehl, G. Kiel, C.P. Köhler, H. Spiering, P. Gütlich, Inorg. Chem. 25 (1986) 1565.
[41] S. Decurtins, P. Gütlich, C.P. Köhler, H. Spiering, A. Hauser, Chem. Phys. Lett. 105 (1984) 1.
[42] A. Hauser, Chem. Phys. Lett. 192 (1992) 65.
[43] C. Bruns-Yilmaz, J. Kusz, H. Spiering, P. Gütlich (1999) to be published.
[44] J.D. Eshelby, Solid State Physics, vol. 3, Academic, New York, 1956, p. 79.
[45] A. Bousseksou, J. Nasser, J. Linares, K. Boukheddaden, F. Varret, J. Phys. I 2 (1992) 1381.